8-1-2018

# Application of Fractal Dimension for Quantifying Noise Texture in Computed Tomography Images

P. Khobragade
*Marquette University*

Jiahua Fan
*GE Healthcare*

Franco Rupcich
*GE Healthcare*, franco.rupcich@marquette.edu

Dominic J. Crotty
*GE Healthcare*

Taly Gilat Schmidt
*Marquette University*, tal.gilat-schmidt@marquette.edu

Accepted version. *Medical Physics*, Vol. 45, No. 8 (August 2018): 3563-3573. DOI. 

*Medical Physics*, Vol. 45, No. 8 (August 2018): 3563-3573. DOI. 

# Application of Fractal Dimension for Quantifying Noise Texture in Computed Tomography Images

P. Khobragade
Department of Biomedical Engineering, Marquette University and Medical College of Wisconsin, Milwaukee, WI
Jiahua Fan
GE Healthcare, Waukesha, WI
Franco Rupcich
GE Healthcare, Waukesha, WI
Dominic J. Crotty
GE Healthcare, Waukesha, WI
Taly Gilat Schmidt
Department of Biomedical Engineering, Marquette University and Medical College of Wisconsin, Milwaukee, WI

# Abstract

## Purpose

Evaluation of noise texture information in CT images is important for assessing image quality. Noise texture is often quantified by the noise power spectrum (NPS), which requires numerous image realizations to estimate. This study evaluated fractal dimension for quantifying noise texture as a scalar metric that can potentially be estimated using one image realization.

## Methods

The American College of Radiology CT accreditation phantom (ACR) was scanned on a clinical scanner (Discovery CT750, GE Healthcare) at 120 kV and 25 and 90 mAs. Images were reconstructed using filtered back projection (FBP/ASIR 0%) with varying reconstruction kernels: Soft, Standard, Detail, Chest, Lung, Bone, and Edge. For each kernel, images were also reconstructed using ASIR 50% and ASIR 100% iterative reconstruction (IR) methods. Fractal dimension was estimated using the differential box-counting algorithm applied to images of the uniform section of ACR phantom. The two-dimensional Noise Power Spectrum (NPS) and one-dimensional-radially averaged NPS were estimated using established techniques. By changing the radiation dose, the effect of noise magnitude on fractal dimension was evaluated. The Spearman correlation between the fractal dimension and the frequency of the NPS peak was calculated. The number of images required to reliably estimate fractal dimension was determined and compared to the number of images required to estimate the NPS-peak frequency. The effect of Region of Interest (ROI) size on fractal dimension estimation was evaluated. Feasibility of estimating fractal dimension in an anthropomorphic phantom and clinical image was also investigated, with the resulting fractal dimension compared to that estimated within the uniform section of the ACR phantom.

## Results

Fractal dimension was strongly correlated with the frequency of the peak of the radially averaged NPS curve, having a Spearman rank-order coefficient of 0.98 (*P*-value < 0.01) for ASIR 0%. The mean fractal dimension at ASIR 0% was 2.49 (Soft), 2.51 (Standard), 2.52 (Detail), 2.57 (Chest), 2.61 (Lung), 2.66 (Bone), and 2.7 (Edge). A reduction in fractal dimension was observed with increasing ASIR levels for all investigated reconstruction kernels. Fractal dimension was found to be independent of noise magnitude. Fractal dimension was successfully estimated from four ROIs of size 64 × 64 pixels or one ROI of 128 × 128 pixels. Fractal dimension was found to be sensitive to non-noise structures in the image, such as ring artifacts and anatomical structure. Fractal dimension estimated within a uniform region of an anthropomorphic phantom and clinical head image matched that estimated within the ACR phantom for filtered back projection reconstruction.

## Conclusions

Fractal dimension correlated with the NPS-peak frequency and was independent of noise magnitude, suggesting that the scalar metric of fractal dimension can be used to quantify the change in noise texture across reconstruction approaches. Results demonstrated that fractal dimension can be estimated from four, 64 × 64-pixel ROIs or one 128 × 128 ROI within a head CT image, which may make it amenable for quantifying noise texture within clinical images.


# 1 Introduction

Quantifying noise in CT images is important for evaluating image quality and optimizing scan techniques.**1**-**7** The noise in a CT image can be described by both its magnitude and texture. Noise standard deviation is a simple scalar metric used to measure the noise magnitude in the image. However, noise standard deviation does not fully describe the noise properties. Images with the same noise standard deviation may have different noise textures that affect image quality.**8**, **9** Noise texture is determined by the correlation of intensity between neighboring pixels and is affected by the reconstruction kernel used in filtered back projection and also by iterative reconstruction methods.**8**, **9**

The Noise Power Spectrum (NPS) is a Fourier-domain metric that provides information about the noise power at each spatial frequency. The integral of the NPS equals the noise variance.**10**, **11** The shape of the NPS determines the contribution of each spatial frequency to the noise, thus describing the noise texture. NPS with higher concentration in the lower spatial frequencies results in noise with a coarse appearance, while NPS concentration in the higher frequency range results in a grainier noise texture.**6**, **8**, **9**

Nonlinear iterative reconstruction methods have been shown to produce different noise textures compared to images reconstructed by filtered back projection (FBP).**12**, **13** Previous studies reported shifting of the NPS toward the lower spatial frequencies and reduction in noise magnitude when reconstructed with iterative algorithms by different CT vendors.**9**, **14**, **15**

Reliable metrics for quantifying noise texture may be useful for comparing and optimizing image reconstruction approaches. While the NPS describes noise texture, it requires numerous image realizations and is a multidimensional quantity. Scalar metrics of noise texture that can be estimated using fewer images and a smaller region of interest (ROI) may be useful for comparing reconstruction algorithms and tuning algorithm parameters. By assuming radial symmetry, the NPS has been represented as a one-dimensional (1D) curve and used to analyze texture information.**9** The frequency at which the peak of the 1D NPS curve occurs has been used as a scalar descriptor of noise texture information for matching reconstruction kernels across vendors.**9** An advantage of the NPS-peak frequency as a noise texture metric is that it is an absolute metric in units of spatial frequency. However, finding the NPS-peak frequency requires numerous images to first estimate the NPS.

As NPS requires numerous image realizations for estimation, it is typically estimated using a uniform test phantom for which many ROIs are available. However, iterative reconstruction approaches may exhibit nonlinear behavior, such that image quality may vary locally depending on image structure. A scalar metric of noise texture that can be estimated within a single, small region of interest may make it possible to evaluate noise texture within uniform regions of clinical images.

The purpose of this study was to investigate fractal dimension as a scalar metric of noise texture. Previous studies applied fractal dimension as a feature for tissue classification tasks such as carcinoma detection**16** and bone growth assessment.**17** A previous study demonstrated the challenges of estimating the fractal dimension of a texture from a discrete image.**18** The estimated fractal dimension was found to vary with the sampling and quantization of the image and the box sizes (scales) used for estimation. While the accuracy of the absolute value of fractal dimension was found to depend on the estimation conditions, the estimated fractal dimension varied monotonically with true fractal dimension. The results of this previous study suggest that fractal dimension may be a useful relative metric for comparing the noise texture of different reconstruction approaches. Thus, the purpose of our study was to evaluate the ability of fractal dimension to quantify differences in noise texture between different reconstruction approaches.

In this study, using phantom images of varying noise texture reconstructed using different algorithms, fractal dimension was validated against the previously proposed scalar metric of the frequency of the NPS peak (NPS-peak frequency).**9** Fractal dimension may be advantageous for noise texture quantification in clinical applications if it can be estimated using less image information than that of the NPS-peak frequency. To investigate this potential advantage of fractal dimension, this study compared the number of ROIs required to estimate fractal dimension compared to NPS-peak frequency. The effect of ROI size and pixel size on fractal dimension estimation was also investigated. The feasibility of estimating fractal dimension within an anthropomorphic phantom image and a clinical image was also investigated by comparing the resulting fractal dimension to that estimated using a uniform phantom.

# 2 Materials and methods

## 2.A. Fractal dimension estimation

Fractals are complex patterns that exhibit self-similarity, meaning that the pattern is composed of repeating structures that are similar across different scales. For a bounded set, *A,* in Euclidean space, the fractal dimension, *D*, is defined as

$$D = \frac{\log(N_r)}{\log\left(\frac{1}{r}\right)},$$

$$D = \frac{\log(N_r)}{\log\left(\frac{1}{r}\right)}, \quad (1)$$

where *r* is a scaling factor and $N_r$ is the number of distinct copies of A, scaled by *r*, needed to completely cover the set A. The fractal dimension, *D*, can be calculated for fractals with deterministic self-similarity. For objects with statistical self-similarity, numerous algorithms have been proposed to estimate the fractal dimension.19, 20 Fractal dimension has been shown to correlate well with the perceived visual roughness of a surface, with *D* = 2 corresponding to a smooth surface and *D* = 3 corresponding to maximum roughness, where roughness is a subjective descriptor of the irregularity and variation in a surface. In CT imaging, the noise texture may be smooth (i.e., less rough) or grainy (i.e., rougher) depending on the reconstruction method.

Variations of the differential box-counting (DBC) algorithm have been used to estimate fractal dimension for gray scale images.**20**-**22** The basic idea of these algorithms is to consider the gray scale image as a three-dimensional surface and to estimate the number of boxes needed to represent the surface for different box sizes, where the number of boxes and box size are related to $N_r$ and *r* in Eq. **1**, respectively. This paper used the modified differential box-counting algorithm proposed by Liu et al.,**23** which is briefly described here. Details of the full algorithm can be found in Liu et al.**23**

Assume a gray scale image of size *M* × *M* pixels with *G* total gray levels. To estimate fractal dimension, the given *M* × *M* image is partitioned into nonoverlapping square regions of size *s* × *s*, where *s* is an integer. The partition size *s* is related to the scaling factor, *r* in Eq. **1**, by

$$s = Mr$$

$$s = Mr \quad (2)$$

For each scaling factor *r*, the intensity of the gray levels is also discretized into units of s',

$$s' = Gr$$

$$s' = Gr \quad (3)$$

Using this process, the three-dimensional surface represented by the gray scale image is partitioned into boxes of size *s* × *s* × *s*'. For each scaling factor *r*, $N_r$ is estimated as the total number of boxes needed to cover this three-dimensional surface using the algorithm presented in Liu et al.**23** The algorithm presented in Liu et al.**23** includes a shifting step along the intensity direction to reduce quantization errors. The algorithm also includes a one-pixel shift of the two-dimensional (2D) grid of boxes in the image plane to avoid undercounting in the presence of edges. For a deterministic fractal, the relationship between $\log(N_r)$ and $\log(1/r)$ is linear, with

fractal dimension defined as the slope, as in Eq. 1. After performing the differential box-counting algorithm, the fractal dimension of an image is estimated as the slope of the best fit line relating the estimated $\log(N_r)$ to the investigated scale factors, $\log\left(1/r\right)$ as determined by linear regression. An important parameter in the box-counting algorithm is range of box sizes used to estimate fractal dimension. We performed a study to identify a robust range of box sizes as will be described in Section **2.D**. As described in Section **2.G**, fractal dimension was estimated in ROIs of varying sizes. Throughout our investigation, the standard deviation of an estimated fractal dimension value was determined as the standard deviation of fractal dimension estimates obtained from multiple sets of ROIs.

## 2.B. Noise power spectrum and correlation with fractal dimension

The NPS-peak frequency was previously suggested as a scalar metric of noise texture.**9** In this work, the correlation between fractal dimension and NPS-peak frequency was evaluated to validate the fractal dimension metric against the established metric of NPS-peak frequency.

The 2D NPS, *NPS*(*u,v*) of an image ROI, *I*(*x,y*), was calculated as

$$NPS(u,v) = \frac{\Delta x \Delta y}{N_x N_y} |FT[I(x,y) - \bar{I}]|^2$$

$$NPS(u,v) = \frac{\Delta x \Delta y}{Nx Ny} |FT[I(x,y) - \bar{I}]|^2 \quad (4)$$

using previously published methods,9, 11, 24-26 where *u*, *v* represent spatial frequency ($mm^{-1}$) in the *x* and *y* direction, respectively. $N_x$ and $N_y$ are the number of pixels in the *x* and *y* direction and $\Delta_x$ and $\Delta_y$ are the pixel dimensions (mm). In Eq. 4, FT denotes the Fourier transform of the selected ROI, $I(x,y)$ minus the mean value of the ROI, $\bar{I}$. Subtracting the mean value of the ROI forces the zero-frequency level of the power spectrum to zero.

For each investigated reconstruction approach, the 2D *NPS*(*u,v*) was normalized by its integral, resulting in the normalized 2D *NPS,* denoted by *nNPS*(*u,v*). Normalization was performed to evaluate the shape of the *NPS*. After normalization, the 1D representation of *nNPS*(*r*) was calculated by radial binning the *nNPS*(*u,v*) to 256 discrete integer bins, assuming radial symmetry of *nNPS*(*u,v*). The frequency of the peak of the 1D *NPS* curve was determined as the reference scalar metric of noise texture. The standard deviation of the NPS-peak frequency was estimated as the standard deviation of NPS-peak values obtained from multiple sets of ROIs.

The fractal dimension and NPS-peak frequency were estimated for each reconstruction approach listed in Table 1 using 300 ROIs of size 128 × 128 pixels. ROIs were equally distributed across five positions in the ACR phantom, as shown in Fig. 1. The agreement between the fractal dimension and NPS-peak frequency was evaluated with the Spearman rank-order correlation test, which measures the strength and direction of the monotonic relationship between two variables.

**Table 1.** Image acquisition parameters

| | **NPS calculation and fractal dimension** |
|---|---|
| Tube voltage | 120 kV |
| Tube current time product | 20, 25 and 90 mAs |
| Reconstruction FOV | 200 mm |
| Slice thickness | 0.625 mm |
| Number of slices | 300 |
| Reconstructed pixel size | 0.39 × 0.39 mm |

| | |
|---|---|
| Reconstruction algorithm | FBP (ASIR 0%), ASIR 50%, and ASIR 100% |
| Reconstruction kernels | Soft, Standard, Detail, Chest, Lung, Bone, Edge |

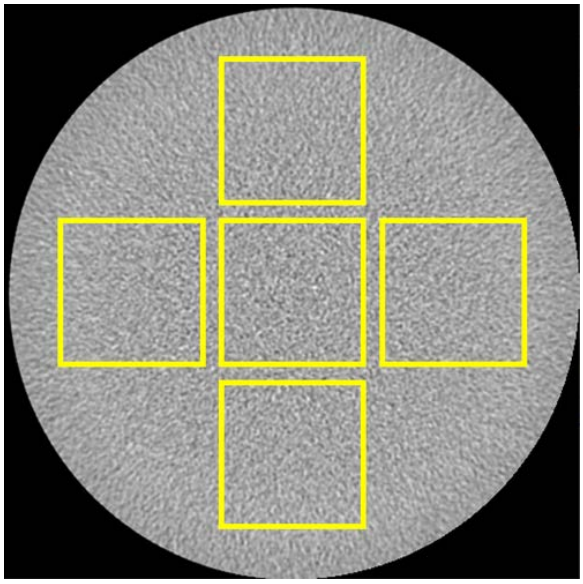

**Figure 1** Location of extracted 128 × 128 pixel ROIs within ACR phantom. [Color figure can be viewed at wileyonlinelibrary.com]

## 2.C. Image acquisition

To investigate fractal dimension as a metric of noise texture, the uniform section of module three of the ACR CT phantom was scanned on a clinical scanner (Discovery CT750, GE Healthcare) at 120 kV. To produce images with varying noise texture, images were reconstructed using FBP (ASIR 0%) with different reconstruction kernels: Soft, Standard, Detail, Chest, Lung, Bone, and Edge. For each kernel, images were also reconstructed using ASIR 50% and ASIR 100% IR methods. Image acquisition parameters are shown in Table 1.

## 2.D. Selection of box sizes for fractal dimension estimation

A previous study highlighted the importance of selecting a robust set of box sizes for estimating fractal dimension and the importance of keeping the quantization and range of box sizes constant across different conditions for which fractal dimension will be compared.**18** While there is no standard rule for choosing the box sizes, previous studies suggest excluding very small and large boxes relative to the ROI size.**21**, **27** Increasing the maximum box size increases the number of data points that are available for estimating the slope of the relationship in Eq. 1, potentially improving the accuracy and robustness of the fractal dimension estimate. However, larger box sizes may not be appropriate for estimating the fractal dimension of a texture.**18**, **21** A smaller maximum box size would enable estimating fractal dimension within smaller ROIs, which would be beneficial for quantifying texture in clinical images.

We performed a study to identify the smallest range of box sizes that provided robust fractal dimension estimation for the reconstructed CT images. The box-counting algorithm was performed on 300 ROIs of size 256 × 256 pixels for images reconstructed with ASIR 0% and the Edge kernel (grainiest noise texture) and ASIR 100% with the Soft kernel (smoothest noise texture). Fractal dimension was estimated with box sizes of $s = 2^i$, with $i$ representing consecutive integers between 1 and $i_{max}$. To determine a robust range of box sizes, $i_{max}$ was varied between 2 and 7. $FD_j$ refers to the fractal dimension estimated with $i_{max} = j$. The final value of $i_{max}$ was selected as the one for which fractal dimension changed by less than 3% when the additional larger box size was incorporated into the estimation (i.e., $FD_j/FD_{j-1} > 0.97$) for both reconstruction approaches.

## 2.E. The effect of noise magnitude on fractal dimension

A quantitative metric of noise texture should ideally be independent of the noise magnitude. To test the hypothesis that fractal dimension is independent of noise magnitude, the fractal dimension was estimated for images reconstructed with filtered back projection with the Soft, Standard, Detail, Chest, Lung, Bone, and Edge kernels at 25 and 90 mAs. Although noise texture can change with dose for nonlinear reconstruction algorithms and/or at extreme dose levels, the experimental conditions in this study were selected to result in equivalent noise texture for the ACR phantom and filtered back projection reconstruction. For each dose level, fractal dimension was estimated and averaged from 300, 128 × 128 pixel ROIs.

## 2.F. The effect of number of ROIs on fractal dimension estimation

Fractal dimension will have potential advantages as a noise texture metric if it can be estimated from a small number of images relative to the number required to reliably calculate the reference metric of NPS-peak frequency. To investigate the relationship between the noise texture metrics and number of image realizations, the fractal dimension and the NPS-peak frequency were estimated using the methods described in Sections **2.A** and **2.B** with the number of ROIs used for estimation varying from 1 to 300. In this study, the ROI size was fixed at 128 × 128 pixels. To improve the robustness of NPS-peak frequency estimation from 50 or fewer ROIs, the 1D NPS curves were filtered with a 9-point Gaussian kernel prior to identification of the NPS peak.

## 2.G. Effect of ROI size on fractal dimension estimation

Variability in the local *NPS* has been observed depending on the estimation parameters such as ROI size and number of ROIs.**25** For *NPS*, increasing the ROI size increases the spatial frequency resolution of the *NPS*; however, fewer ROIs may be available for *NPS* calculation, which can lead to errors. For fractal dimension, increasing the ROI size increases the number of scale factors, $r$, that are considered, thereby providing more data points for estimating the slope of the linear relationship in Eq. **1**, as was investigated in the study described in Section **2.D**. Larger ROI sizes also provide more boxes at each scale, thereby reducing uncertainty in the box counts. To estimate the effect of ROI size on fractal dimension, ROIs of sizes: 64 × 64, 128 × 128, and 256 × 256 pixels were extracted from the uniform ACR phantom images and fractal dimension was estimated from the 300 ROIs of each size. For the 128 × 128 and 256 × 256 ROIs, fractal dimension was estimated with $i_{max}$ = 6, based on the analysis described in Section **2.D**. For the smaller ROI size of 64 × 64, the maximum box size was limited to half of the ROI size to ensure the division of the ROI into a minimum of four boxes ($i_{max}$ = 5).

## 2.H. Effect of pixel size on fractal dimension

The reconstructed field of view (FOV) changes the effective pixel size when the number of pixels is kept constant. In the absence of noise-aliasing effects, changing the pixel size should not alter the noise texture. The noise texture may change for larger pixel sizes for which aliasing occurs. We investigated whether fractal dimension was affected by pixel size for a case with negligible noise aliasing. Images of the ACR phantom were reconstructed using FBP (Standard kernel) and FOV of 20 and 30 cm, corresponding to pixel sizes of 0.39 × 0.39 mm and 0.59 × 0.59 mm, respectively. At 20 cm FOV with the Standard kernel, the noise power was zero for frequencies greater than 0.86 lp/mm. Therefore, both investigated pixel sizes meet the Nyquist criteria to avoid noise aliasing. Fractal dimension and NPS-peak frequency were estimated using 300, 128 × 128 pixel ROIs and compared for the two different pixel size settings. For both cases, fractal dimension was estimated using box sizes of $2^i$, with $i$ ranging from two to six. This range of box size was chosen based on analysis performed in Section **2.D**.

## 2.I. Investigation of fractal dimension estimation in an anthropomorphic phantom and clinical image

A noise texture metric that can be estimated in a single, small ROI would potentially enable quantifying noise texture within clinical images. To investigate the feasibility of quantifying noise texture in an anthropomorphic phantom and clinical image, we tested the agreement between the fractal dimension estimated in a uniform region of an anthropomorphic phantom and clinical image to the reference fractal dimension estimated in the uniform ACR phantom. An anthropomorphic CT phantom (CTU-41, Kyoto Kagaku) was scanned at 90 mAs on a clinical scanner (Discovery CT750, GE Healthcare). To produce images with varying noise texture, the phantom images were reconstructed using the reconstruction methods listed in Table 1. Fractal dimension was also estimated in a clinical head CT image acquired at 120 kV and 285 mA (Discovery CT750, GE Healthcare). The phantom and clinical head images used in this study are shown in Fig. 2. The clinical data were reconstructed using pixel size and slice thickness listed in Table 1 and with the Standard and Bone kernels with ASIR 0%, ASIR 50%, and ASIR 100%. For both the anthropomorphic phantom and clinical image, fractal dimension was estimated in four 64 × 64 ROIs and a 128 × 128 pixel ROI extracted from a uniform region in the brain area as shown in Fig. 2. Fractal dimension values estimated in the anthropomorphic phantom and clinical images were compared to the fractal dimension estimated in the uniform ACR phantom. For filtered back projection, which is a linear algorithm, we expect similar fractal dimension values when estimated using the ACR phantom or a uniform region of an anthropomorphic image. Therefore, this experiment will validate the fractal dimension values estimated within the uniform region of an anthropomorphic phantom and clinical image. Once validated for filtered back projection, the fractal dimension estimates within the anthropomorphic phantom can be used to investigate changes in noise texture due to local structure when using nonlinear iterative reconstruction approaches.

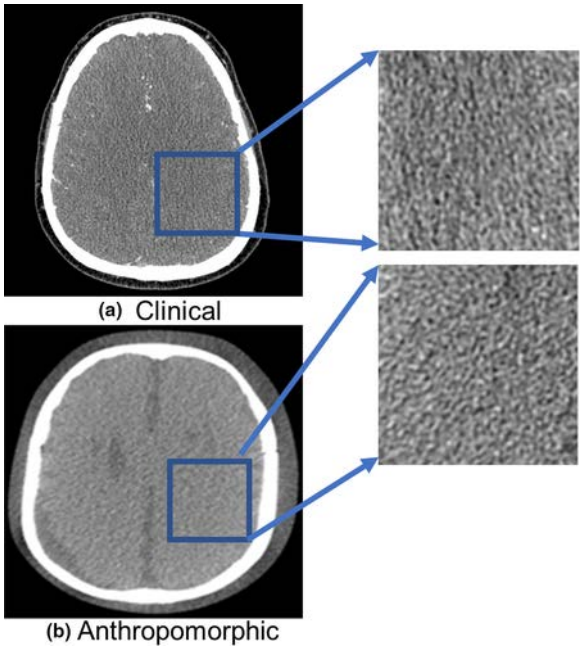


**Figure 2** (a) Clinical and (b) phantom head image demonstrating the extracted 128 × 128 pixel ROIs that were used for fractal dimension estimation. [Color figure can be viewed at wileyonlinelibrary.com]

# 3 Results

## 3.A. Selection of box sizes for fractal dimension estimation

Figures 3(a) and 3(b) plot the fractal dimension estimated using different ranges of box sizes ($s = 2^i$) for the Edge kernel with ASIR 0% and the Soft kernel with ASIR 100%. Increasing the maximum box size increases the number of data points that are available for estimating the slope of the relationship in Eq. 1. The results in Fig. 3 demonstrate an increase in the estimated fractal dimension with increasing range of box sizes for both reconstruction methods. A key observation is that the estimation of fractal dimension became more stable as the range of box sizes increased. A maximum box size of 64 ($i = 6$) was selected for subsequent studies, as the change in fractal dimension was less than 3% when this box size was added to the range used for estimation.

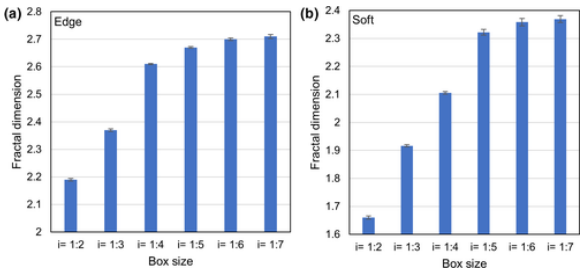


**Figure 3** Fractal dimension estimated at varying ranges of box sizes for images reconstructed by (a) Edge kernel ASIR 0% and (b) Soft kernel ASIR 100%. Error bars represent the standard deviation of fractal dimension estimated across 300 ROIs. [Color figure can be viewed at wileyonlinelibrary.com]

## 3.B. Fractal dimension for different reconstruction approaches

Example ROIs extracted from the reconstructed images are shown in Fig. 4, demonstrating the change in noise texture with different kernels and different percentages of ASIR. To facilitate comparison of noise texture across reconstruction approaches, the intensities in each ROI were normalized by the standard deviation of the ROI and all images are displayed at the same window width and level. The fractal dimension and NPS-peak frequency are displayed for each image, both calculated as the average across 300 ROIs. Noise texture appeared smoother for images reconstructed using a higher percentage of ASIR, which corresponded to a decrease in fractal dimension and NPS-peak frequency for each kernel. Grainer noise texture was observed in images reconstructed using the Lung and Bone kernels, which generally corresponded to an increase in NPS-peak frequency and fractal dimension.

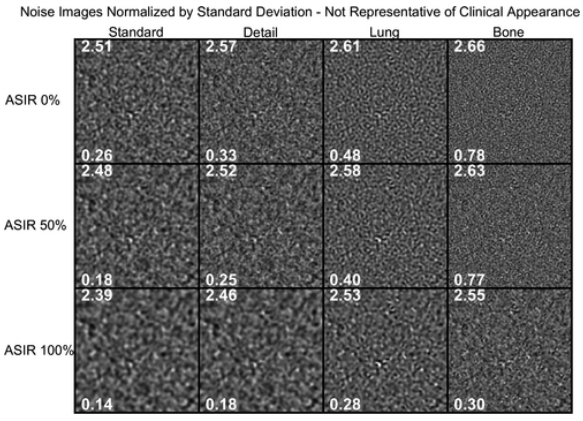


**Figure 4** ROIs from the images reconstructed with FBP (ASIR 0%), ASIR 50%, and ASIR 100% with reconstruction kernels of Standard, Detail, Lung, and Bone, which span the range of textures seen across all kernels. This figure contains a subset of the studied kernels so that the displayed ROIs are large enough to depict the noise texture.

A high-resolution figure that includes the ROIs from all investigated kernels is available in the Supporting Information for this manuscript. The estimated fractal dimension and NPS-peak frequency ($mm^{-1}$) are displayed at the top and bottom of each image, respectively. To facilitate comparison of texture, all ROIs were normalized by their standard deviation and are displayed at a window of ±5 standard deviations from the mean. Please note that due to this normalization, the images appear differently than the typical clinical presentation. The reduction in noise magnitude seen with an increase in ASIR percentage is not visible due to this normalization. Depiction of textures may require viewing on a high-resolution display device.

The estimated fractal dimensions for the varying reconstruction kernels and ASIR percentages are plotted in Fig. 5, demonstrating the variation in fractal dimension with reconstruction approach. For each reconstruction kernel, ASIR 0% resulted in the highest fractal dimension, while ASIR 100% resulted in the lowest fractal dimension.

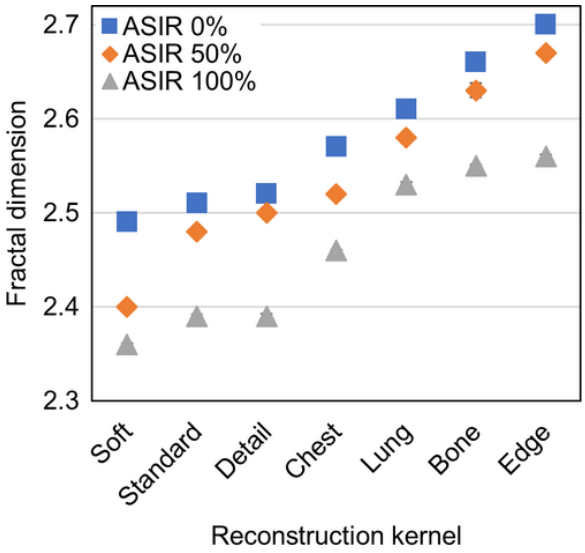


**Figure 5** Fractal dimension estimated from images reconstructed by different kernels using ASIR 0%, ASIR 50%, and ASIR 100%. The error bars represent standard deviation of the fractal dimension across the 300 ROIs. [Color figure can be viewed at wileyonlinelibrary.com]

Ring artifacts were noticeable in the central ROI of some images reconstructed by the Lung kernel at 90 mAs. The ring artifacts increased the correlation between neighboring pixels, thus decreasing the estimated fractal dimension from 2.58 without noticeable ring artifacts to 2.55 with ring artifacts. This result demonstrates that fractal dimension is sensitive to artifacts and other non-noise variations in the image. ROIs reconstructed by the lung kernel that contained visible ring artifacts were manually excluded from analysis.

## 3.C. Correlation between fractal dimension and NPS-peak frequency

The NPS-peak frequency for all investigated reconstruction methods is plotted in Fig. 6. The NPS-peak frequency decreased with increasing ASIR percentage. Figure 7 plots the fractal dimension against the NPS-peak frequency, demonstrating a nonlinear correlation between the two noise texture metrics. The Spearman rank-order correlation coefficient between the two metrics was 0.98 ($P < 0.001$), 0.95 ($P < 0.001$), and 0.93 ($P < 0.001$) for ASIR 0%, ASIR 50%, and ASIR 100%, respectively, signifying a strong monotonic relationship between the two metrics for the investigated reconstruction algorithms.

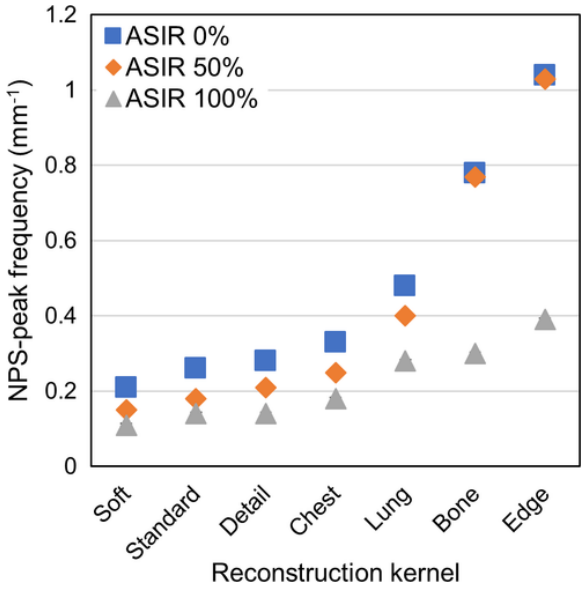


**Figure 6** NPS-peak frequency for different kernels reconstructed using ASIR 0%, ASIR 50%, and ASIR 100%. Error bars represent the standard deviation in NPS-peak frequency. [Color figure can be viewed at wileyonlinelibrary.com]

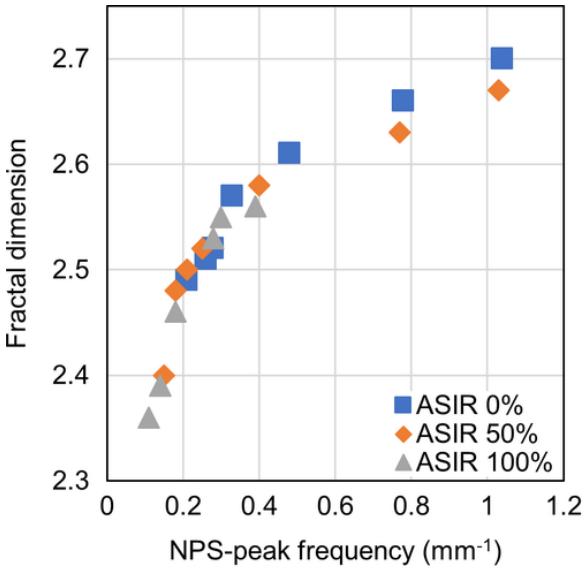


**Figure 7** Fractal dimension plotted against the NPS-peak frequency for ASIR 0%, ASIR 50%, and ASIR 100% demonstrating a positive correlation between the two metrics. [Color figure can be viewed at wileyonlinelibrary.com]

The nonlinear relationship between fractal dimension and NPS-peak frequency demonstrates that fractal dimension is more sensitive to changes in texture in smoother images, while NPS-peak frequency is more sensitive to changes in texture in grainier images.

## 3.D. Effect of noise magnitude on fractal dimension

Figure 8 plots the fractal dimension at 25 and 90 mAs for the images reconstructed by filtered back projection for all investigated kernels. As demonstrated in Fig. 8, fractal dimension was minimally affected by noise magnitude.

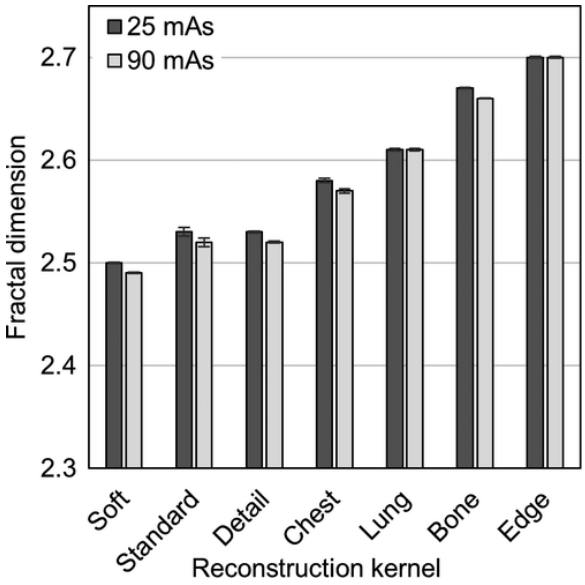


**Figure 8** Fractal dimension estimated at 25 and 90 mAs for images reconstructed with ASIR 0%.

## 3.E. The effect of number of ROIs on fractal dimension estimation

The variation in the fractal dimension and NPS-peak frequency with respect to the number of ROIs used for estimation is plotted in Figs. 9(a) and 9(b) for filtered back projection reconstruction and two levels of ASIR reconstruction with the Standard kernel. Similar results were obtained for the other investigated reconstruction approaches. The fractal dimension varied by less than 2% as the number of ROIs decreased from 300 to 1. With the applied Gaussian smoothing of the 1D NPS curves, 20 or more ROIs were required to estimate the NPS-peak frequency with less than 4% error. The standard deviation of both the fractal dimension and NPS-peak frequency estimates increased with increasing ASIR percentage.

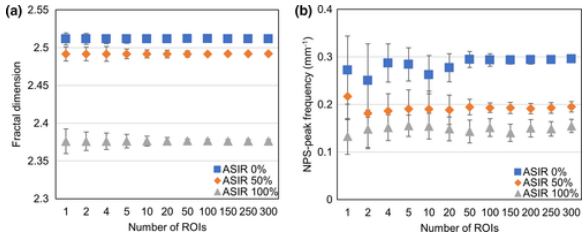


**Figure 9** Variation in the (a) fractal dimension and (b) NPS-peak frequency estimated using varying numbers of ROIs from images reconstructed using the Standard kernel and ASIR 0%, ASIR 50%, and ASIR 100%. Error bars represents standard deviation across multiple trials. [Color figure can be viewed at wileyonlinelibrary.com]

## 3.F. Effect of ROI size on fractal dimension estimation

Figure 10(a) plots the fractal dimension estimated from different ROI sizes for ASIR 0%, ASIR 50%, and ASIR 100% reconstructed with the Standard kernel. As expected, based on the results of the box size study in Section **3.A**., fractal dimension was not reliably estimated for ROI sizes less than 128 × 128, due to the limited number of box sizes available for estimating the linear relationship in Eq. 1. However, smaller ROI sizes would be beneficial for estimating noise texture in clinical images. In the case of the 128 × 128 pixel ROI, the largest box size used for fractal dimension estimation is of size 64 × 64 pixels. Therefore, we also investigated combining four separate 64 × 64 pixel ROIs to form a larger 128 × 128 ROI for fractal dimension estimation. Figure 10(b) plots the fractal dimension estimated from different sized ROIs, where four 64 × 64 ROIs were combined to form a larger ROI, demonstrating that fractal dimension can be reliably estimated by combining four 64 × 64 ROIs. The results

suggest that fractal dimension for representing noise texture can be estimated from four 64 × 64 pixel ROIs or one 128 × 128 pixel ROI.

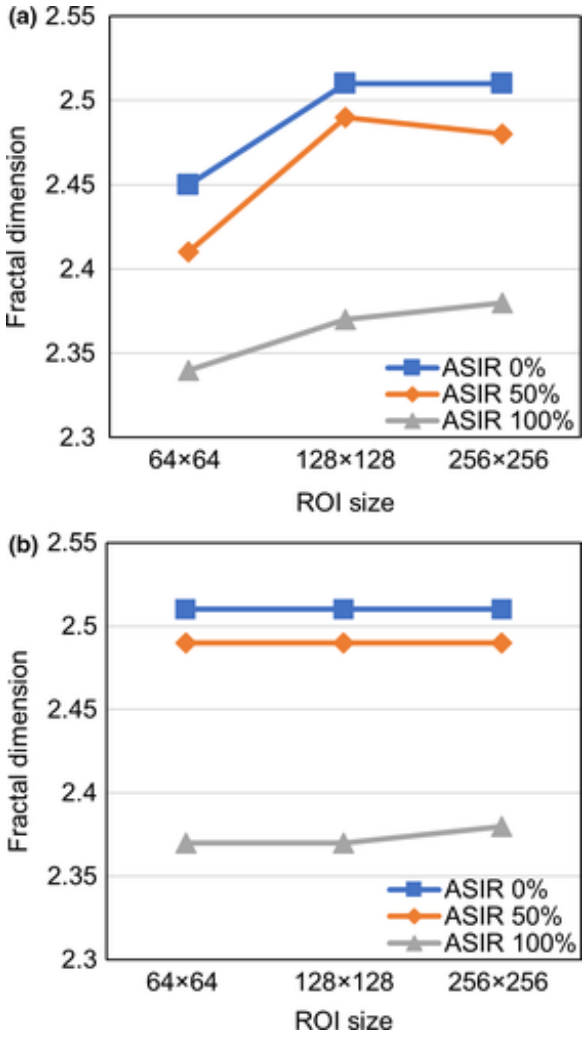


**Figure 10** Both plots display fractal dimension estimated from different ROI sizes for three reconstruction approaches. (a) shows the results using ROIs of size 64 × 64 pixels, while (b) shows the results of combining four ROIs of size 64 × 64 pixels into a larger ROI for fractal dimension estimation. For all cases, 300 total ROIs were used for estimation for each case. [Color figure can be viewed at wileyonlinelibrary.com]

## 3.G. Effect of pixel size on fractal dimension

Figures 11(a) and 11(b) display ROIs extracted from the ACR phantom reconstructed at FOV of 20 and 30 cm, respectively. Fractal dimension increased by less than 1% and NPS-peak frequency increased by 4% when the pixel size increased, which is within the range of fractal dimension and NPS-peak frequency uncertainty.

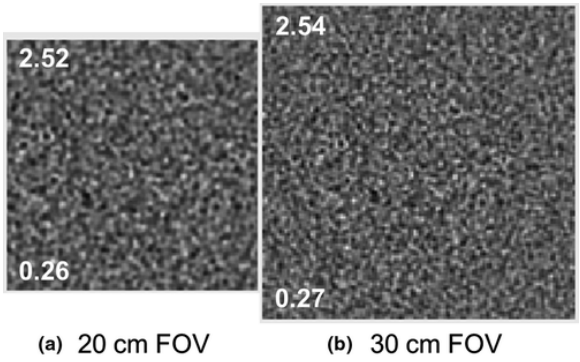


**Figure 11** ROIs extracted from ACR phantom reconstructed at (a) 20 cm FOV (0.39 × 0.39 mm pixel size) and (b) 30 cm FOV (0.59 × 0.59 mm pixel size). For each ROI, the top label shows the fractal dimension and the bottom label shows the NPS-peak frequency (lp/mm).

## 3.H. Investigation of fractal dimension estimation in an anthropomorphic phantom and clinical image

Figure **12** plots the fractal dimension estimated from a 128 × 128 pixel ROI in the uniform region of the brain in an anthropomorphic phantom and clinical head CT image, along with the fractal dimension estimated from a 128 × 128 region of the ACR phantom, for different reconstruction kernels, and ASIR percentages. For the filtered back projection reconstruction (ASIR 0%) and ASIR 50%, the fractal dimension estimated in the anthropomorphic phantom and clinical image were equivalent to that estimated in the uniform phantom.

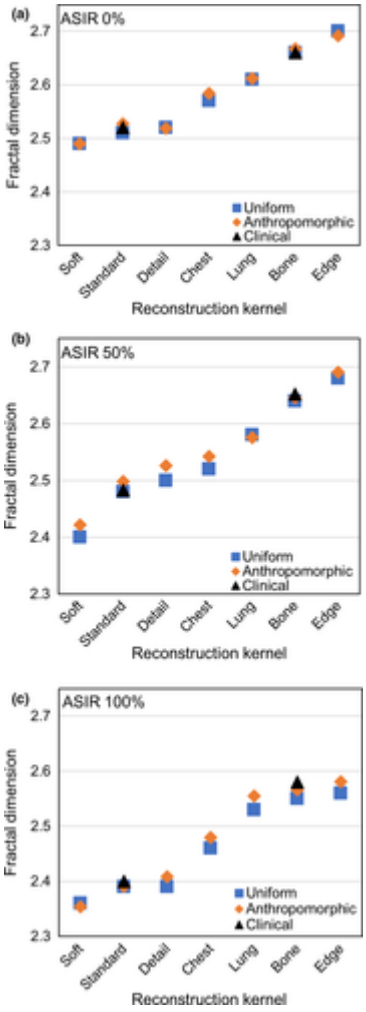


**Figure 12** Fractal dimension calculated from the uniform ACR phantom and uniform ROIs extracted from the brain region of an anthropomorphic phantom and clinical head CT image for varying reconstruction kernels at (a) ASIR 0%, (b) ASIR 50%, and (c) ASIR 100%. The clinical head CT image was reconstructed using only the standard and bone kernels. [Color figure can be viewed at wileyonlinelibrary.com]

For ASIR 100%, the fractal dimension was slightly higher when estimated in the clinical image and anthropomorphic phantom for the higher frequency kernels, such as the Bone kernel as shown in Fig. **12**(c), although this change is within the expected uncertainty of the fractal dimension estimation. Figure **13** displays the fractal dimension estimated at three different 128 × 128 ROIs within the brain region, where two of the ROIs contain primarily uniform background and the third ROI contains anatomical structure. The estimated fractal dimension remained constant (2.51 and 2.52) for the two uniform ROIs located in different brain regions. As expected, the fractal dimension was sensitive to anatomical structure, resulting in an estimated fractal dimension of 2.36. This result demonstrates the importance of selecting a uniform region of the object. Fractal dimension was also estimated using four 64 × 64 pixel ROIs within different uniform regions of the brain that were combined to form a larger ROI. The resulting fractal dimension was 2.52, which agreed with the fractal dimension estimated from the 128 × 128 pixel ROI.

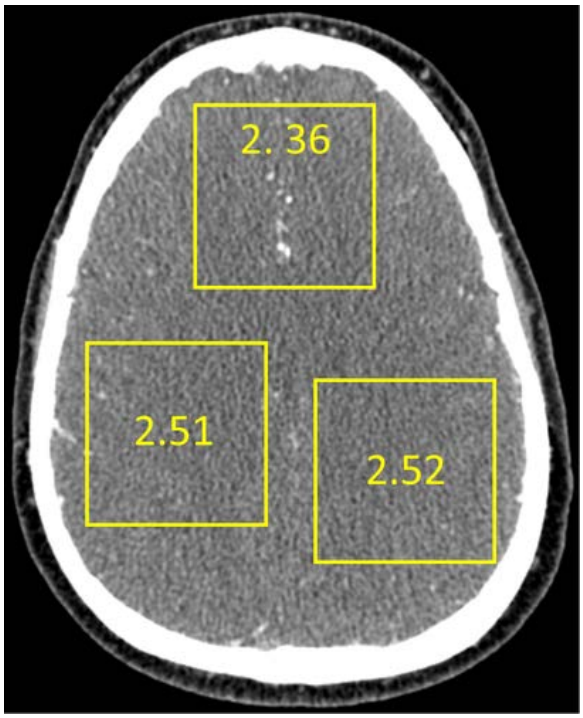


**Figure 13** Fractal dimension estimated at three different 128 × 128 pixel ROIs in a clinical head CT image. [Color figure can be viewed at wileyonlinelibrary.com]

## 4 Discussion

This study demonstrated the application of fractal dimension as a scalar metric for quantifying noise texture across different reconstruction kernels and levels of ASIR reconstruction. The results demonstrated that fractal dimension was strongly correlated to the previously proposed scalar metric of NPS-peak frequency, with a Spearman rank-order correlation coefficient of 0.98 ($P < 0.001$), 0.95 ($P < 0.001$), 0.93 ($P < 0.001$) for ASIR 0%, ASIR 50%, and ASIR 100%, respectively. The correlation between fractal dimension and peak frequency is valid for the specific iterative reconstruction algorithms evaluated in this study; further investigation is needed for generalization to other nonlinear reconstruction algorithms. Fractal dimension was underestimated for images reconstructed with ASIR 100% and high-frequency kernels, causing the reduction in Spearman correlation coefficient for ASIR 100%. This underestimation of fractal dimension appears to be caused by the increase in outlier noise intensities in these cases, which may be due to the combination of the noise amplification by the high-frequency noise kernels and the nonlinear response of the iterative algorithm. The modified differential box-counting algorithm used in this study is one approach for estimating fractal dimension. Other estimation algorithms have been found to be less sensitive to outliers and may be beneficial to investigate for noise texture quantification in future studies.**28** Despite the underestimation of fractal dimension for the combination of high-frequency kernels and ASIR 100% reconstruction, fractal dimension represented the trend in grainer noise texture for higher frequency kernels and a fixed ASIR percentage, while also representing the trend of smoother noise texture for a fixed kernel and increasing ASIR percentage.

The estimation of fractal dimension was found to be sensitive to artifacts and non-noise variations in the image, such as ring artifact and anatomical structure as shown in Fig. **13**. Therefore, for fractal dimension to quantify noise texture, the ROI must be carefully selected such that noise is the dominating source of variation. As seen in Fig. **7**, although fractal dimension exhibited a positive correlation to NPS-peak frequency, the relationship between the two metrics was nonlinear. The nonlinear relationship between fractal dimension and NPS-peak frequency plotted in Fig. **7** demonstrates that fractal dimension is more sensitive to changes in texture in

smoother images, while NPS-peak frequency is more sensitive to changes in texture in grainier images. The fractal dimension metric could be transformed to linearly correlate with the peak-NPS frequency. However, additional investigation and human observer studies are needed to understand the how well these metrics represent the perception of noise texture by the human visual system.

As a scalar quantity, fractal dimension does not provide information about the orientation of the noise texture and would not be appropriate for quantifying directional noise correlations. This is a general limitation of scalar noise texture metrics. Estimating 1D fractal dimension along different orientations may provide a method for quantifying texture orientation and would be an interesting area of future work.

As in previous studies,**18** the fractal dimension values estimated in this study varied when the range of box sizes used for estimation was small ($i_{max} < 6$). This result demonstrates the importance of using a constant range of box sizes when comparing different noise textures. This study determined that fractal dimension can be estimated from four ROIs of size 64 × 64 pixels, suggesting that fractal dimension may be suitable for evaluating noise texture in the clinical setting where estimation is limited by the available number and size of uniform regions. In this study, the feasibility of estimating fractal dimension in an anthropomorphic phantom and clinical head CT was demonstrated. For filtered back projection reconstruction, the fractal dimension was equivalent when estimated from the uniform ACR phantom and the uniform region of the brain. This result is expected because filtered back projection is a linear operation that is independent of the object. The results in Section **3.H** demonstrate a slight increase in fractal dimension for ASIR100% when estimated in the anthropomorphic phantom and clinical image compared to the uniform phantom for the higher frequency reconstruction kernels. Fractal dimension was consistent across different ROIs in the uniform region of the clinical head CT image. However, anatomical structure in the ROIs can change the estimated fractal dimension, as shown in Fig. **13**. Hence, careful selection of ROIs will be required to reliably estimate fractal dimension within clinical images. A limitation of this study is that only a single head CT image was used to demonstrate feasibility of calculating fractal dimension in clinical images. Additional studies with a larger number of clinical images are needed.

The ability to quantify noise texture using fewer images and within a single region of a clinical image may have several applications. Fractal dimension could be used to compare and match the noise texture of different reconstruction approaches. Fractal dimension could also be used to investigate the effect of nearby object structure on the noise texture for nonlinear reconstruction algorithms. Fractal dimension could potentially be incorporated within iterative reconstruction approaches to optimize, constrain, or match the noise texture to a reference value.

# 5 Conclusion

Fractal dimension was investigated as a scalar metric of noise texture for images reconstructed with varying reconstruction kernels and iterative reconstruction strengths. Fractal dimension correlated with the frequency of the peak of the 1D NPS curve and was independent of noise magnitude, suggesting that the scalar metric of fractal dimension can be used to quantify the change in noise texture across reconstruction approaches. The results demonstrated that fractal dimension can be estimated from a single ROI of size 128 × 128 pixels or four ROIs of size 64 × 64 pixels. The fractal dimension estimated within a uniform region of a clinical image was equivalent to that estimated from the uniform phantom for filtered back projection reconstruction. The results suggest that fractal dimension may be beneficial and practical for quantifying noise texture within anthropomorphic phantom and clinical images.

## Conflicts of Interest

Parag Khobragade and Taly Gilat Schmidt receive research funding from GE Healthcare. Jiahua Fan, Franco Rupcich, and Dominic Crotty are employees of GE Healthcare.

## Reference


1Pachon JH, Yadava G, Pal D, Hsieh J. Image quality evaluation of iterative CT reconstruction algorithms: a perspective from spatial domain noise texture measures. In: Medical Imaging 2012: Physics of Medical Imaging. International Society for Optics and Photonics; 2012. page 83132K.

2Solomon JB, Li X, Samei E. Relating noise to image quality indicators in CT examinations with tube current modulation. *Am J Roentgenol*. 2013; **200**: 592– 600.

3Sagara Y, Hara AK, Pavlicek W, Silva AC, Paden RG, Wu Q. Abdominal CT: comparison of low-dose CT with adaptive statistical iterative reconstruction and routine-dose CT with filtered back projection in 53 patients. *Am J Roentgenol*. 2010; **195**: 713– 719.

4Moscariello A, Takx RAP, Schoepf UJ, et al. Coronary CT angiography: image quality, diagnostic accuracy, and potential for radiation dose reduction using a novel iterative image reconstruction technique—comparison with traditional filtered back projection. *Eur Radiol*. 2011; **21**: 2130.

5Hou Y, Liu X, Xv S, Guo W, Guo Q. Comparisons of image quality and radiation dose between iterative reconstruction and filtered back projection reconstruction algorithms in 256-MDCT coronary angiography. *Am J Roentgenol*. 2012; **199**: 588– 594.

6Boedeker KL, Cooper VN, McNitt-Gray MF. Application of the noise power spectrum in modern diagnostic MDCT: part I. Measurement of noise power spectra and noise equivalent quanta. *Phys Med Biol*. 2007; **52**: 4027.

7Li K, Tang J, Chen G-H. Noise performance of statistical model based iterative reconstruction in clinical CT systems. In: Medical Imaging 2014: Physics of Medical Imaging. International Society for Optics and Photonics; 2014. page 90335J.

8Boedeker KL, McNitt-Gray MF. Application of the noise power spectrum in modern diagnostic MDCT: part II. Noise power spectra and signal to noise. *Phys Med Biol*. 2007; **52**: 4047– 4061.

9Solomon JB, Christianson O, Samei E. Quantitative comparison of noise texture across CT scanners from different manufacturers. *Med Phys*. 2012; **39**: 6048– 6055.

10Riederer SJ, Pelc NJ, Chesler DA. The noise power spectrum in computed x-ray tomography. *Phys Med Biol*. 1978; **23**: 446.

11 International Commision of Radiation Units and Measurement. Medical imaging—the assessment of image quality. ICRU Report No 54 (ICRU publication, Washington, DC; 1996). 1997.

12Richard S, Husarik DB, Yadava G, Murphy SN, Samei E. Towards task-based assessment of CT performance: system and object MTF across different reconstruction algorithms. *Med Phys*. 2012; **39**: 4115– 4122.

13Wilson JM, Christianson OI, Richard S, Samei E. A methodology for image quality evaluation of advanced CT systems. *Med Phys*. 2013; **40**: 031908.

14Ghetti C, Palleri F, Serreli G, Ortenzia O, Ruffini L. Physical characterization of a new CT iterative reconstruction method operating in sinogram space. *J Appl Clin Med Phys*. 2013; **14**: 263– 271.

15Samei E, Richard S. Assessment of the dose reduction potential of a model-based iterative reconstruction algorithm using a task-based performance metrology. *Med Phys*. 2014; **42**: 314– 323.

16Kido S, Kuriyama K, Higashiyama M, Kasugai T, Kuroda C. Fractal analysis of internal and peripheral textures of small peripheral bronchogenic carcinomas in thin-section computed tomography: comparison of bronchioloalveolar cell carcinomas with nonbronchioloalveolar cell carcinomas. *J Comput Assist Tomogr*. 2003; **27**: 56– 61.

17Khobragade P, Jain A, Nagesh SVS, et al. Micro-Computed tomography (CT) based assessment of dental regenerative therapy in the canine mandible model. In: Medical Imaging 2015: Biomedical Applications

in Molecular, Structural, and Functional Imaging. International Society for Optics and Photonics; 2015. page 94171D.
18Huang Q, Lorch JR, Dubes RC. Can the fractal dimension of images be measured? *Pattern Recogn*. 1994; **27**: 339– 349.
19Pentland AP. Fractal-based description of natural scenes. *IEEE Trans Pattern Anal Mach Intell*. 1984; **6**: 661– 674.
20Sarkar N, Chaudhuri BB. An efficient differential box-counting approach to compute fractal dimension of image. *IEEE Trans Syst Man Cybern*. 1994; **24**: 115– 120.
21Bisoi AK, Mishra J. On calculation of fractal dimension of images. *Pattern Recognit Lett*. 2001; **22**: 631– 637.
22Li J, Du Q, Sun C. An improved box-counting method for image fractal dimension estimation. *Pattern Recognit*. 2009; **42**: 2460– 2469.
23Liu YU, Chen L, Wang H, Jiang L, Zhang Y, Zhao J, et al. An improved differential box-counting method to estimate fractal dimensions of gray-level images. *J Vis Commun Image Represent*. 2014; **25**: 1102– 1111.
24Dobbins JT, Samei E, Ranger NT, Chen Y. Intercomparison of methods for image quality characterization. II. Noise power spectrum. *Med Phys*. 2006; **33**: 1466– 1475.
25Dolly S, Chen H, Anastasio M, Mutic S, Li H. Practical considerations for noise power spectra estimation for clinical CT scanners. *J Appl Clin Med Phys*. 2016; **17**: 392– 407.
26Dobbins JT III. Image quality metrics for digital systems. *Handb Med Imaging*. 2000; **1**: 161– 222.
27Buczkowski S, Kyriacos S, Nekka F, Cartilier L. The modified box-counting method: analysis of some characteristic parameters. *Pattern Recognit*. 1998; **31**: 411– 418.
28Gneiting T, Ševčíková H, Percival DB. Estimators of fractal dimension: assessing the roughness of time series and spatial data. *Stat Sci*. 2012; **27**: 247– 277.

## Supporting Information

| Filename | Description |
|---|---|
| mp13040-sup-0001-FigS1.tifTIFF image, 2.2 MB | **Fig. S1.** Region of Interest from the images reconstructed with FBP (ASIR 0%), ASIR 50%, and ASIR 100% with reconstruction kernels of Soft, Standard, Chest, Detail, Lung, Bone, and Edge. |
| mp13040-sup-0002-caption.docxWord document, 10.5 KB | |

Region of Interest from the images reconstructed with FBP (ASIR 0%), ASIR 50%, and ASIR 100% with reconstruction kernels of Soft, Standard, Chest, Detail, Lung, Bone, and Edge. The estimated fractal dimension and NPS-peak frequency ($mm^{-1}$) are displayed at the top and bottom of each image, respectively. To facilitate comparison of texture, all ROIs were normalized by their standard deviation and are displayed at a window of +/- 5 standard deviations from the mean. Please note that due to this normalization, the images appear differently than the typical clinical presentation. The reduction in noise magnitude seen with an increase in ASIR percentage is not visible due to this normalization. Depiction of textures may require viewing on a high-resolution display device.

Noise Images Normalized by Standard Deviation - Not Representative of Clinical Appearance